Flow field-flow fractionation/multiangle light scattering of sodium hyaluronate from various degradation processes

Myeong Hee Moon [a],*, Da Young Shin [a], Namkoo Lee [a], Euijin Hwang [b], Il-Hwan Cho [b]

[a] *Department of Chemistry, Yonsei University, Seoul 120-749, South Korea*
[b] *Department of Biotechnology, Shinpoong Pharmaceutical, Co. Ltd., Ansan, Kyeonggi-Do, South Korea*

Abstract

Sodium hyaluronate (NaHA) is an ultrahigh molecular weight polysaccharide that is found in body tissues, synovial fluid, the vitreous humor, and the umbilical cord, and the size characterization of NaHA is important in pharmaceutical applications. On-line field-flow fractionation/multiangle light scattering/differential refractive index (FlFFF/MALS/DRI) has been applied for the study of degradation efficiency of sodium hyaluronate (NaHA). A NaHA raw sample was degraded by different chemical or physical methods and the degraded NaHA samples were separated using field-programming FlFFF, in which separation is achieved by differences in diffusion coefficients or hydrodynamic diameters. Separation was followed by serial detection using MALS and DRI. Molecular weight distribution (MWD) and information relating to the radius of gyration of the NaHA samples were examined for the raw and degraded NaHA samples. Samples studied include: two different products of ultrasonic degradation, two products of alkaline degradation, and four different products of enzymatic degradation. While alkaline degradation showed a moderate degradation compared to ultrasonic and enzymatic methods in reducing average MW, the latter two degradation methods showed significant changes in average molecular weight and in conformation of NaHA.
© 2008 Elsevier B.V. All rights reserved.

1. Introduction

Sodium hyaluronate (NaHA), a sodium salt of hyaluronic acid (HA) or hyaluronan, is an ultrahigh molecular weight (10^5 to 10^7) aqueous polysaccharide composed of a disaccharide repeating unit (D-glucuronic acid and *N*-acetyl-D-glucosamine) linked by a β(1-4)-glycosidic bond [1–5]. HA is found in the skin, synovial fluid, umbilical cord, vitreous humor, and the cartilage [6] of the human body, and industrial HA is obtained from bacterial cultures or from animal bodies. Due to its biological safety and rheological characteristics, intact or degraded forms of HA have been used for medical or pharmaceutical applications such as knee joint injections for osteoarthritis, ophthalmic surgery, and as a skin moisturizer [7–10]. The unique characteristics of HA make these applications possible. HA can, for example, absorb large amounts of water. Furthermore, HA plays

an important role in the organization and integrity of the extracellular matrix by preserving its form; it also aids in the spatial arrangement of tissue due to its visco-elastic properties [11,12]. Depending on the needs of the application such as for cosmetics, the substitutes in ophthalmic surgery, or the treatment of knee joint disease, an intact or degraded form of HA are utilized.

In general, degradation of polymers has conventionally been accomplished by ultrasonication which induces a mechanical force resulting in depolymerization [13]. In ultrasonication, it is generally accepted that small bubbles generated by rapid pressure variation from the propagation of acoustic energy induces chain scission in polymers by the generation of large velocity gradients during formation and collapse of bubbles. It has been reported that ultrasonication can be utilized to prepare HA of a desired molecular weight and narrow MW distribution (MWD) [12]. Besides ultrasonication, degradation can also be initiated with enzymes, alkaline solutions, thermal energy, and gamma radiation. Recently, the ability to predict the stability of crosslinked HA gels has been reported using testicular hyaluronidase [11], which is known to break β(1-4) linkage by

* Corresponding author. Tel.: +82 2 2123 5634; fax: +82 2 364 7050.
E-mail address: mhmoon@yonsei.ac.kr (M.H. Moon).

hydrolysis. Alkaline degradation of polysaccharides is known to occur with a cleavage of glycosidic linkages at the reducing terminus, and a recent report on alkaline degradation of molasses has been shown to produce de-icers [14]. In our earlier work, irradiation of HA using gamma rays was shown to produce a significant decrease in MW with a narrow MWD [15]. In optimizing the degradation process for the industrial use of HA, accurate characterization of MW and MWD as well as conformational information is necessary. While size exclusion chromatography (SEC) has been used for determining MW of HA [16,17], it is often beyond the limit of separation to handle ultrahigh MW polymers due to the limitation in pore sizes of the packing materials, the possibility of shear-induced degradation of ultralarge molecules, a lack of appropriate standards needed for calibration, and a possible column blocking.

As a complementary method, flow field-flow fractionation (FlFFF) can be utilized for the size separation and characterization of MW and MWD of aqueous polymers with on-line coupling of multiangle light scattering (MALS) along with a differential refractive index (DRI) detector. FlFFF is a size fractionation technique similar to SEC yet provides the capability of handling broader and larger macromolecules or even micronto nano-sized particles in an open unpacked channel space and separation of polymers based on the hydrodynamic diameter and shape [18–22]. Hyphenation of FlFFF with MALS has been shown to be effective to obtain MW values and conformational information of macromolecules with materials such as modified cellulose, polysaccharide gum Arabic and pullulan [23–26]. The first approach to resolve HA by FlFFF was tried by Wahlund and Litzen [27] to show the possibility of size fractionation with an asymmetrical FlFFF channel and, later FlFFF/MALS of HA was attempted by Takahashi et al. [8]. Recently, Moon and coworkers [28] investigated the efficiency of field-programmed separation in Frit inlet asymmetrical FlFFF (FI-AFlFFF) for HA analysis and applied the method to study the effect of sample dissolution temperature and gamma radiation degradation on the size and conformation of NaHA [15,29,30].

In this article, we study the degradation efficiency of NaHA by linear field programming FI-AFlFFF coupled with MALS/DRI. Studies were focused to evaluate the variation of average molecular weight, MWD, and conformation of degraded NaHA products in solution which were made by ultrasonic, enzymatic, and alkaline degradation by varying parameters.

2. Experimental

2.1. Materials and reagents

The degraded NaHA samples used in this study were prepared by Shinpoong Pharm. Co. Ltd. (Ansan, Korea) from raw NaHA which was extracted from rooster comb. Degradation of NaHA uses the same raw NaHA solution, specifically, 5 g/L in 0.3 M NaCl solution. For alkaline degradation, the raw material was treated with 0.3 M NaOH solution (pH 13.5) for 6 and 8 h. Enzymatic degradation was obtained by adding testicular hyaluronidase (EC 3.2.1.35) at different units and periods of time: 2 U/0.5 h, 2 U/1 h, 5 U/0.5 h, and 5 U/1 h. For ultrasonic

degradation, the raw NaHA solution was sonicated for 4 and 8 h at 20 kHz, 20 W and 4 °C. After degradation, each degraded product was precipitated by the addition of ethanol and was then freeze-dried. NaHA samples were dissolved at a concentration of 0.8–1.0 mg/mL in a carrier solution, 0.1 M NaNO$_3$ that is used for FlFFF separation in this study, at 4 °C overnight without stirring in order to prevent any degradation. Prepared sample solution was stored in a refrigerator and a volume of 20 μL was injected for all runs.

2.2. FFF/MALS/DRI

The FlFFF channel used was the frit inlet asymmetrical FlFFF (FI-AFlFFF), which was the same as used in an earlier study [15]. The FI-AFlFFF channel dimensions were 27.2 cm × 0.0170 cm (length × thickness) with an initial breadth of 2.0 cm and a final breadth of 1.0 cm (trapezoidal), and a geometrical volume of 0.70 cm^3. The channel space was made by clamping a Mylar spacer, which was cut to the above dimensions, with two plastic blocks. One block was installed with a ceramic frit for the accumulation wall to allow for crossflow exiting, and the other block (depletion wall side) was equipped with a short frit (3.0 cm from the sample inlet) at the beginning end of the channel. Through the small inlet frit, a high-speed flow stream (frit flow) was delivered to provide a hydrodynamic relaxation of the sample components entering the channel with the sample injection stream. At the accumulation wall of channel, a regenerated cellulose membrane (PLCGC with 10,000 MWCO, from Millipore Corp. Billerica, MA, USA) was placed to keep the sample components from penetrating through the frit by the movement of crossflow.

For FlFFF separation of NaHA samples, carrier liquid (0.1 M NaNO$_3$ solution prepared from de-ionized water) was delivered to both the sample inlet and the frit inlet using two HPLC pumps, a Model 305 HPLC pump from Gilson (Villers Le Bell, France) and a Model M930 HPLC pump from Young-Lin Co. (Seoul, Korea), respectively. The latter pump was used for programming frit flow rate, which was decreased by linear field decay programs. Two different programming programs were used depending on the broadness of the molecular weight distribution of the degraded NaHA sample. In decay program-I, the initial frit flow rate (set as identical to crossflow rate in this study) began with 2.0 mL/min for 3 min and then decreased linearly to 0.5 mL/min over 5 min, to 0.1 mL/min over 11 min, further to 0.02 mL/min over 5 min and then, finally, was maintained at 0.02 mL/min until the end of separation. Decay program-II began with 4 min of initial delay at 2.0 mL/min and then the initial flow rate decreased to 0.5 mL/min over 6 min, to 0.1 mL/min over 10 min and then, finally, was maintained at 0.1 mL/min until the end of separation. For the outflow leading to the detectors, the same flow rate (0.10 mL/min) was utilized for all runs.

Sample injection was made through Model 7125 loop-type injector valve from Rheodyne (Cotati, CA, USA), with a loop volume of 20 μL. Eluted sample components were monitored by two serial detectors: a DAWN-DSP multiangle light scattering detector at a wavelength of 632.8 nm and an Optilab DSP differential refractive index (DRI) detector at a wavelength of 690 nm from Wyatt Technology (Santa Barbara, CA, USA). In order to

remove any fluctuation in flow rate at the channel outlet during crossflow programming, a syringe pump, Model PN1610 Syringe Dosing System from Postnova Analytics (Lansberg, Germany), was placed in unpump mode at the end of the DRI detector. For the MALS detector, calibration was performed with filtered toluene and normalization was performed with albumin (BSA). The dn/dc values of NaHA samples were measured with an Optilab DSP interferometric refractometer with respect to concentration variation; this calculation was made using DNDC5 software from Wyatt Technology. The calculated value of dn/dc for the raw NaHA sample was 0.142. For the MW calculation, the DRI fractogram was baseline adjusted by subtracting the baseline of each blank run using CORONA software from Wyatt Technology. This was essential to adjust the shift of detector baseline which was observed during field programming. Results were also corrected for inter-detector time delay (inter-detector volume as 0.12 mL). MW calculations from the two combined detector signals were made by the manufacturer's ASTRA software using a third-order polynomial fit according to the Berry method of the Debye plot as suggested in the literature [31]. However, for the smaller MW species which were degraded significantly, a first-order fit was used instead. Since the signals at the third angle fluctuated substantially when measured for ultrahigh MW components, only LS signals of the 4–10th angles were processed in using the Berry method.

3. Results and discussion

3.1. Ultrasonic degradation of NaHA

Ultrasonication is known to generate mechanical energy in solution by forming and collapsing bubbles very rapidly [13], and is expected to break NaHA chains into shorter lengths or possibly to loosen the multiply folded helical NaHA chain structures. Fig. 1 represents the FlFFF fractograms of the control sample and the two products degraded by ultrasonication over 4 and 8 h. The three main fractograms in the center of Fig. 1 are the MALS signals recorded at 90°, while the lower section of the figure provides the DRI signals. FlFFF fractionations of NaHA samples (control and two products) were made with the two different crossflow field programmings (or decay programs) depending on the molecular weight distributions, specifically decay programs-I and -II (details are provided in the experimental section above and volumetric flow rate as a function of time is plotted in the top portion of Fig. 1).

The control sample (represented by black circles) was fractionated by field programming in Fl-AFlFFF using field decay program-I, in which all of the NaHA molecules are expected to achieve size-based separation. This can be confirmed by plotting the MW values which are calculated for each volume slice of FlFFF elution vs. retention time. The calculated MW values following the same notation (black circles) to represent LS signals of the same sample are superimposed with LS signals, and they show the gradual increase of MW values as retention time increases. This result indicates that the size fractionation of the control NaHA sample is properly made at an increasing order of MW. The calculated MW values of the control sample appear to
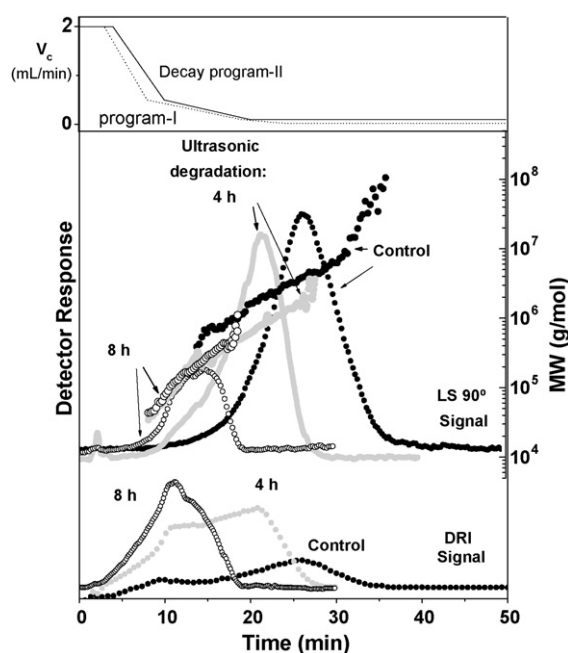

Fig. 1. FlFFF fractograms (DRI signals at the bottom and MALS at 90°) of NaHA samples from ultrasonic degradation and MW values calculated at each retention time slice. FlFFF separation of the control sample was carried out by field decay program-I and the two degraded samples were run by decay program-II, both of which are provided at the top of the figure.

span up to ∼10⁸ g/mol. When the same experiment was applied to the ultrasonicated NaHA samples at varying sonication times (4 and 8 h), the elution profile of the degraded NaHA products were significantly different from that of the control sample, such that the longer sonication process shifted the retention of NaHA molecules to shorter time scales. Based on this result, the depolymerization or degradation of NaHA molecules has effectively been made by ultrasonication.

For the two degraded products shown in Fig. 1, decay program-II was employed for separation in FlFFF. Since these two samples contain smaller MW NaHA molecules generated from sonication, they need a longer period for delaying the initial field strength to resolve smaller MW components in the Fl-AFlFFF channel. While the two degraded products showed a similar program of MW plots, three facts are evident. As sonication time increases, retention time of the degraded species shifted to shorter time scale, the apparent average MW of the degraded sample decreases, and the intensity of LS signals for the degraded products significantly decreases. However, the DRI signal intensity increases with an increase in sonication time, which is the opposite of the trend observed for LS signals. This phenomenon originates from the fact that the LS detector relies on both MW and concentration, while DRI only relies on the concentration of the sample. Therefore, the observed increase of DRI signal intensity for the degraded products supports the degradation of polymers into shorter MW chains.

MWD of each degraded product was plotted in comparison with the MWD of the control NaHA sample in Fig. 2a. As shown, a clear difference exists in MWD depending on the applied ultrasonic energy. Additional calculated data are listed in Table 1 with
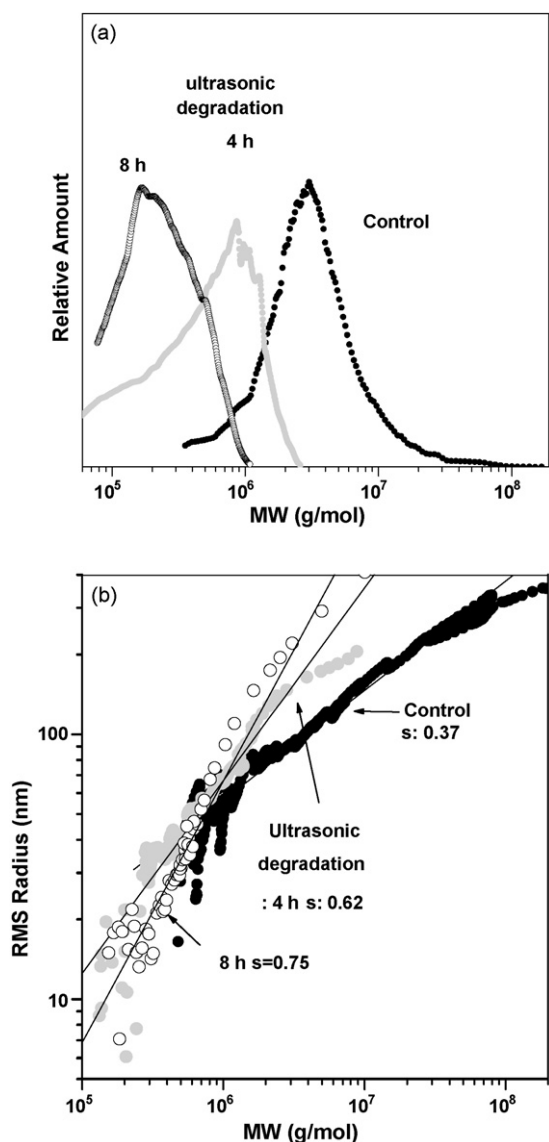
Fig. 2. (a) Comparison of MWDs of the NaHA before and after ultrasonic degradation and (b) plots of RMS radius vs. MW values for the three NaHA samples.

weight average molecular weight (Mw), number average MW (Mn), polydispersity, and average of root mean square (RMS) radius values for the three samples. These results show that 8 h of ultrasonication induced a significant decrease in average MW by ∼25 times, however, the polydispersity values did not change much (from 2.06 for the control sample to 1.91 for the 8 h sample). Average RMS radius decreases to a great extent after ultrasonic degradation. Since the relationship between the RMS radius value of a polymer and its MW allows for the prediction of the structure of polymers used in solution, RMS radius values for the three NaHA samples were plotted against the calculated MW values in Fig. 2b. For the control sample, the calculated slope value, $d \log$ (RMS radius) vs. $d \log$ MW, is 0.37 as indicated in the figure. This slope value is similar to what has been previously observed with raw NaHA materials in our earlier study [30], and provides evidence that the molecular structure of the control sample is relatively compact and entangled. In literature, it is known that NaHA in the solid state may exist as a fully extended molecule or a multiply folded helix stabilized by hydrogen bonds between glycosidic-linked monomers [5]. The slope values for the NaHA samples produced from ultrasonic degradation, were calculated to be 0.62–0.75 which support that the conformation of NaHA material was transformed to a less entangled or linear structure from a compact and folded geometry as a result of ultrasonication. The differences of the RMS radius vs. MW plot for the two degraded products can be explained in that same NaHA molecules ($1–6 \times 10^5$ g/mol) of the 8 h sample are expected to have a more extended structure from a prolonged sonication. The slope calculation was based on the entire data points obtained for each sample, however the regression line may not appear to fit all data points since data points are more populated in some MW region.

3.2. Alkaline treatment of NaHA

The raw NaHA sample solution was treated with 0.3 M NaOH (pH 13.5) for varying time periods (6 and 8 h), and the freeze-dried products were re-suspended in the FlFFF carrier solution and were run by FI-AFlFFF/MALS/DRI using decay program-I. In Fig. 3, LS signals of the two degraded products and the same

Table 1
Effect of degradation methods on MW, RMS radius, and R.S.D. values ($n = 4$) of the NaHA control sample

|	Mw	Mn	Mw/Mn	RMS radius (nm)
Control sample	$4.4 \, (\pm 0.1) \times 10^6$	$2.2 \, (\pm 0.02) \times 10^6$	2.06 ± 0.04	107.6 ± 0.9
Ultrasonication				
4 h	$5.3 \, (\pm 0.04) \times 10^5$	$2.5 \, (\pm 0.03) \times 10^5$	2.03 ± 0.03	37.8 ± 0.3
8 h	$1.7 \, (\pm 0.1) \times 10^5$	$9.0 \, (\pm 0.03) \times 10^4$	1.91 ± 0.04	36.1 ± 0.5
Alkali				
6 h	$2.4 \, (\pm 0.1) \times 10^6$	$1.3 \, (\pm 0.01) \times 10^6$	1.79 ± 0.03	101.8 ± 0.1
8 h	$1.5 \, (\pm 0.1) \times 10^6$	$1.0 \, (\pm 0.01) \times 10^6$	1.43 ± 0.01	83.7 ± 0.5
Enzyme				
2 U/0.5 h	$8.2 \, (\pm 0.05) \times 10^5$	$4.1 \, (\pm 0.04) \times 10^5$	2.03 ± 0.03	51.7 ± 0.1
2 U/1 h	$6.7 \, (\pm 0.01) \times 10^5$	$3.3 \, (\pm 0.03) \times 10^5$	1.99 ± 0.02	49.7 ± 0.1
5 U/0.5 h	$9.0 \, (\pm 0.2) \times 10^4$	$6.3 \, (\pm 0.2) \times 10^4$	1.43 ± 0.06	
5 U/1 h	$8.2 \, (\pm 0.1) \times 10^4$	$5.9 \, (\pm 0.1) \times 10^4$	1.39 ± 0.03	
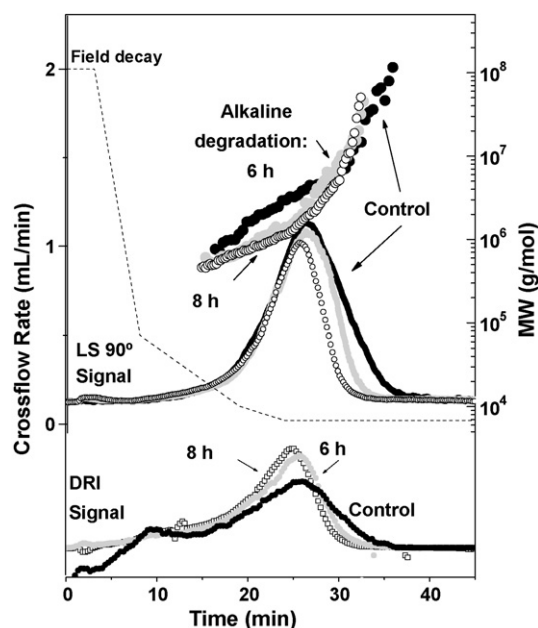
Fig. 3. FlFFF fractograms of a raw NaHA sample superimposed with those of the samples degraded by alkaline exposure at different time periods. Decay program-I was employed. MW values corresponding to each sample are plotted with different symbols but the same symbol convention is used.

control sample are superimposed with the plots of calculated MW values. Sodium hydroxide seemed to degrade polymers to some extent but the differences in the eluted peaks are relatively small even under 8 h of strong base when compared to the significant change observed by ultrasonication. These results show that MW values of the alkaline-treated samples in Fig. 3 increase rather slowly with an increase in retention time up to 25 min. These increases are from the elution of lower MW components which are less entangled, or have extended structure caused by the addition of a strong base. As observed by the slight decrease in the LS signal intensities of the alkaline-treated NaHA samples, the DRI signals of the two NaHA products did not significantly increase from that of the control sample and the peaks did not shift to shorter retention times. From these data it seems that alkaline conditions may not have a strong influence on degradation of NaHA molecules. As shown in Fig. 4, the MWD curves reveal that there are some changes in MWD but changes are relatively small compared to the ultrasonication effect. Calculated M_w values of the alkali 8-h sample is $1.5 (\pm 0.1) \times 10^6$ g/mol as listed in Table 1, and this value is of the same order of magnitude as the control sample (4.4×10^6). RMS radius values decreased to some extent after 8 h of alkaline treatment, and this resulted in a slight increase in the slope value of the plot of log RMS vs. log MW: 0.37 and 0.40 for the 6 and 8 h treated samples, respectively. These results reveal that alkaline degradation is relatively mild and does not significantly change the conformation of NaHA molecules.

3.3. Enzymatic degradation of NaHA

For enzymatic degradation, testicular hyaluronidase was used to react with the NaHA control solution by varying the enzyme

unit per mL of solution: 2 and 5 U/mL. During the enzymatic reaction, reaction time was varied from 0.5 to 1 h. The resulting four degraded NaHA samples (2U-0.5 h, 2U-1 h, 5U-0.5 h, 5U-1 h) were run by FI-AFlFFF/MALS/DRI and all FlFFF fractograms are superimposed in Fig. 5. The first two samples (2U-0.5 h, 2U-1 h) were fractionated using the same field decay program (program-I) used for the control sample, but the remaining samples (5U-0.5 h, 5U-1 h) were resolved using decay program-II as used in Fig. 1. With only 0.5 h of reaction using 2 U/mL of hyaluronidase, the peak (black filled circles) of the degraded NaHA sample (2U-0.5 h) appears to shift significantly to shorter time scales compared to that of the control sample (open circles). A longer treatment (2U-1 h sample) did not result in a considerable shift in retention time, but showed a decrease in LS signal intensity (simultaneous increase in the DRI intensity at the retention time interval of 10–20 min represented by grey circles in Fig. 5), which indicates further degradation. However, when enzyme concentration was increased to 5 U/mL, the LS signals of the two samples (5U-0.5 h and 5U-1 h) were signifi-
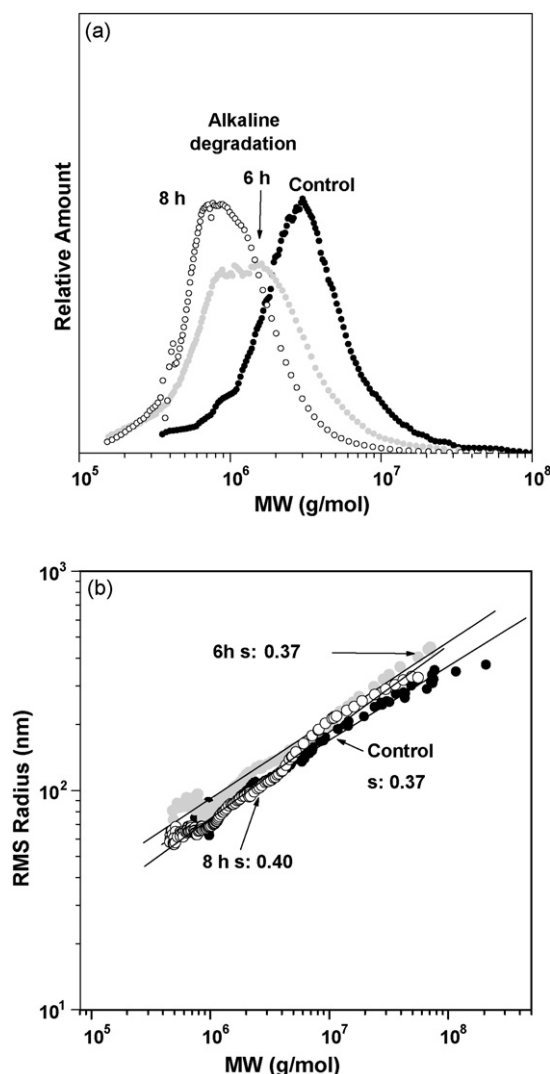

Fig. 4. (a) MWD curves for the alkaline degraded NaHA samples compared to that of the control sample and (b) plots of RMS radius vs. MW values for the alkaline degraded samples.
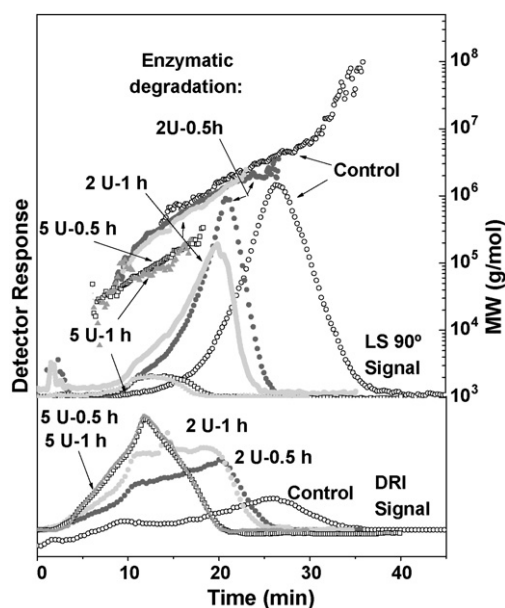
Fig. 5. Effect of enzymatic degradations on the retention of NaHA materials by varying the number of enzyme units and the reaction period. Decay program-I was used for FlFFF separation of the degraded NaHA (2U-0.5 h and -1 h) and program-II was used for the degraded samples (5U-0.5 h and -1 h).
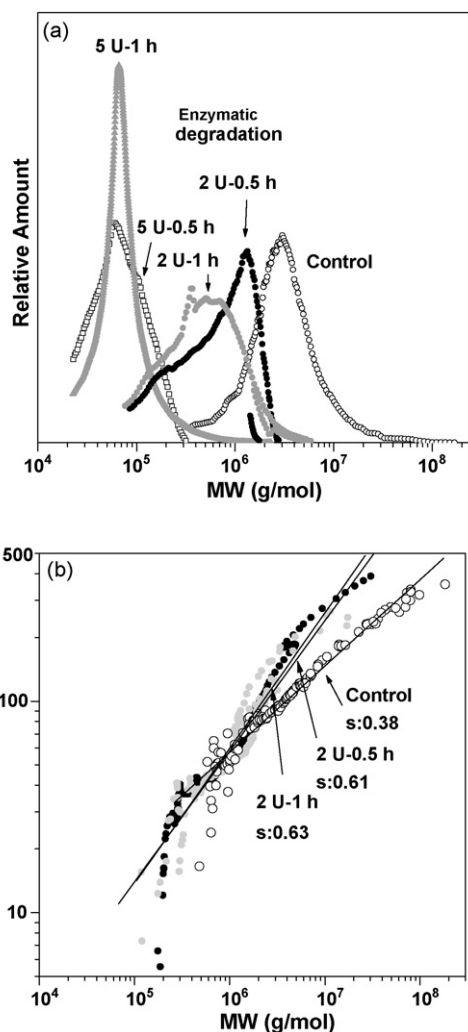

Fig. 6. (a) Influence of enzymatic degradation on MWDs of NaHA samples corresponding to the fractograms shown in Fig. 5, and (b) plots of RMS radius vs. MW values for the enzymatically degraded NaHA products.

cantly reduced and the retention times decreased simultaneously. Decreases in both LS signal intensities and retention times support that the degradation of NaHA molecules was thoroughly made by the increased usage of enzymes. The enhanced degradation is also supported by an increase in DRI signal intensities as well as narrower peak distributions. By comparing the MW values plotted in Fig. 5, it can be seen that NaHA molecules after 5 U treatments are smaller than $\sim 2 \times 10^5$ g/mol. The MW data points for the degraded samples treated with 5 U of enzyme appeared to increase with a decreased slope (open squares and filled triangles in Fig. 5) due to use of the field decay program-II, in which field strength decays more slowly than that of the decay program-I.

MWD curves of the differently degraded products are superimposed in Fig. 6a. As expected from the peaks in Fig. 5, MWD curves of degraded samples are shown to clearly shift to smaller sizes as enzyme concentration increases, and they become narrower with increasing reaction time. Average Mw values listed in Table 1 also show that enzymatic degradation with 2 U resulted in a decrease of Mw to 8.2 (± 0.05) $\times 10^5$ and 6.7 (± 0.01) $\times 10^5$ for 0.5 h and 1 h of reaction, respectively, which are still larger than what can be expected from 4 h of ultrasonication. With the addition of 2 U of enzyme reaction, polydispersity values did not decrease substantially (2.03 and 1.99), while RMS radius values decreased considerably. The calculated values show that the enzyme reaction with 5 U brings a significant breakdown of NaHA chains to much smaller sizes (9.0 (± 0.2) $\times 10^4$ for 5U-0.5 h and 8.2 (± 0.1) $\times 10^4$ for 5U-1 h) with the subsequent decrease in polydispersity values (1.43 and 1.39, respectively).

The slope values of the plots of RMS radius vs. MW values show a clear increase compared to that of the control sample, as shown in Fig. 6b. With 2 U of enzyme reaction, the slope

values are increased to 0.61 and 0.63 as represented in Fig. 6b, indicating that enzymatic degradations also bring unfolding of entangled NaHA molecules to extended structures. However, the similar plots for the samples treated with 5 U were not included in Fig. 6b since uncertainties in the calculation of RMS radius for smaller sizes were large.

4. Conclusions

This study demonstrated the use of FlFFF/MALS/DRI for the evaluation of degradation methods for ultrahigh MW NaHA materials by comparing MWD and conformational variations. While 4–8 h of ultrasonic degradation provides a way to generate NaHA molecules having an average MW of $(1.7–5.3) \times 10^5$ g/mol from the control sample $(4.4 \times 10^6$ g/mol), along with unfolding of compact geometry to more extended structure, alkaline degradation under 0.3 M NaOH for 8 h only gave a small change in average MW $(1.5 \times 10^6$ g/mol) while conformational variation was not found to be significant. Among the three degradation methods utilized

in this study, enzymatic degradation appears to be the most powerful in terms of time-dependent degradation efficiency as well as conformational shift toward linear chain structure. Also, this study showed that a proper field decay program must be selected for FlFFF separation of degraded NaHA materials since molecular weight distribution of NaHA sample varies as degradation proceeds. The present FlFFF/MALS/DRI separation using field programming needs to be improved for speedy separation which can possibly be achieved by using the dual programming method for both outflow rate and crossflow rate.

Acknowledgements

References

[1] B. Yeung, D. Marecak, J. Chromatogr. A 852 (1999) 573.
[2] Z. Iqbal, J.M. Midgley, D.G. Watson, S.D. Karditsas, G.N. Dutton, W. Wilson, Pharm. World Sci. 19 (1997) 246.
[3] K.P. Vercruysse, G.D. Prestwich, Crit. Rev. Ther. Drug Carrier Syst. 15 (1998) 513.
[4] E.D.T. Atkins, C.F. Phelps, J.K. Sheehan, Biochem. J. 128 (1972) 1255.
[5] P. Livant, L. Roden, R. Krishna, Carbohydr. Res. 237 (1992) 271.
[6] G.D. Prestwitch, D.M. Marecak, J.F. Marecek, K.P. Vercurysse, M.R. Ziebel, J. Control. Rel. 53 (1998) 93.
[7] H. Sasari, T.Y. Konttinen, S. Santavirta, Med. Sci. Res. 18 (1989) 99.
[8] R. Takahashi, S. Al-Assaf, P.A. Williams, K. Kubota, A. Okamoto, K. Nishinari, Biomacromolecules 4 (2003) 404.
[9] L.S. Mengher, K.S. Pandher, A.J. Bron, C.C. Davey, Br. J. Opthalmol. 70 (1986) 442.
[10] T. Miyazaki, C. Yomota, S. Okada, J. Ocul. Pharmacol. 12 (1996) 27.
[11] I. Sall, G. Ferad, Polym. Degrad. Stabil. 92 (2007) 915.
[12] T. Miyazaki, C. Yomota, S. Okada, Polym. Degrad. Stabil. 74 (2001) 77.
[13] A.M. Basedow, K. Ebert, Adv. Polym. Sci. 22 (1977) 83.
[14] B.Y. Ynag, R. Montgomery, Bioresour. Technol. 98 (2007) 3084.
[15] D.Y. Shin, E.J. Hwang, I.-H. Cho, M.H. Moon, J. Chromatogr. A 1160 (2007) 270.
[16] N. Motohashi, Y. Nakamichi, I. Mori, H. Nishikawa, K. Umemoto, J. Chromatogr. 435 (1988) 335.
[17] L. Solites, R. Mendichi, E. Machova, B. Steiner, J. Alfoldi, V. Sasinkova, S. Bystricky, K. Balong, Carbohydr. Polym. 39 (1999) 17.
[18] J.C. Giddings, Anal. Chem. 53 (1981) 1170A.
[19] J.C. Giddings, Science 260 (1993) 1456.
[20] M.E. Schimpf, K.D. Caldwell, J.C. Giddings, Field-Flow Fractionation Handbook, Wiley Interscience, NY, 2000.
[21] K.-G. Wahlund, J.C. Giddings, Anal. Chem. 59 (1987) 1332.
[22] S.K. Ratanathanawongs, J.C. Giddings, Anal. Chem. 64 (1992) 6.
[23] B. Wittgren, K.-G. Wahlund, J. Chromatogr. A 791 (1997) 135.
[24] M. Andersson, B. Wittgren, H. Schagerlof, D. Momcilovic, K.-G. Wahlund, Biomacromolecules 5 (2004) 97.
[25] L. Picton, I. Bataille, G. Muller, Carbohydr. Polym. 42 (2000) 23.
[26] C. Duval, D.L. Cerf, L. Picton, G. Muller, J. Chromatogr. B 753 (2001) 115.
[27] K.-G. Wahlund, A. Litzen, J. Chromatogr. A 461 (1989) 73.
[28] H. Lee, H. Kim, M.H. Moon, J. Chromatogr. A 1089 (2005) 203.
[29] H. Kim, H. Lee, M.H. Moon, Bull. Korean Chem. Soc. 27 (2006) 413.
[30] H. Lee, I.-H. Cho, M.H. Moon, J. Chromatogr. A 1131 (2006) 185.
[31] S. Lee, P.-O. Nilsson, G.S. Nilsson, K.-G. Wahlund, J. Chromatogr. A 1011 (2003) 111.